

Supporting Information for

A century-long history of aquatic carbon cycling in the Chesapeake and Delaware Bay Watersheds: modeling lateral transport, burial, and degassing of riverine carbon

Yuanzi Yao¹, Hanqin Tian¹, Shufen Pan¹, Raymond G. Najjar², Marjorie A. M. Friedrichs³,
Zihao Bian¹, Hong-Yi Li⁴, Eileen E. Hofmann⁵

¹International Center for Climate and Global Change Research and School of Forestry and Wildlife Sciences, Auburn University, AL, USA; ²Department of Meteorology and Atmospheric Science, The Pennsylvania State University, University Park, PA, USA; ³Virginia Institute of Marine Science, William & Mary, Gloucester Point, VA, USA; Department of Civil & Environmental Engineering, University of Houston, Cullen College of Engineering, Houston, TX, USA; ⁵Center for Coastal Physical Oceanography, Department of Ocean, Earth and Atmospheric Sciences, Old Dominion University, Norfolk, VA, USA

Contents of this file

Supplementary Methods:

1. Soil Carbon Decomposition

2. Carbon loadings from terrestrial ecosystem to streams

3. Inorganic carbon chemistry

Supplementary Table 1 - 2.

Supplementary Figure 1 -2.

Additional references

Introduction

This supporting information provides methods, figures and tables that are mentioned in the main article.

42 **Supplementary Methods: terrestrial carbon loading**

43 ***1. Soil Carbon Decomposition***

44 DLEM 2.0 defines eleven soil carbon pools, including a dissolved organic matter pool, a woody
45 detritus pool, two litter carbon pools, three microbial pools, and two slow soil organic matter
46 pools, one native organic matter and one passive soil organic matter pool. Several land processes
47 contribute to the organic carbon input to soil including tissue turnover, manure, crop residue, and
48 branch fragmentation, and the associate allocation of carbon and nitrogen following the defined
49 C/N ratio. DLEM can simulate carbon fluxes among the soil pools involving biological
50 decomposition, physical adsorption and desorption, and carbon leaching. The major parameters
51 relevant to the terrestrial carbon loading and in-stream process were summarized in
52 Supplementary Table 2, and the sensitivity analysis can be found in other published work (e.g.,
53 Tian et al., 2012, 2015). In short we found that the 10% changes of key parameters controlling
54 terrestrial carbon loading and riverine carbon processes only resulted in relatively small (overall
55 less than 2%) changes in carbon fluxes, which enhance the confidence of the model performance.
56 The governing equations for estimating soil and litter decomposition use a first-order decay rate
57 constants ($k_{C\ Pool}$), which is influenced by soil temperature, soil water content, nutrient
58 availability, and soil texture:

$$59 \quad k_{C\ Pool} = \frac{k_{max}}{365 \times f(T) \times f(w) \times f(N) \times f(clay)} \quad (1)$$

$$60 \quad f(T) = 4.89 \times e^{-3.432+0.1 \times T \times (1-0.5 \times T/36.9)} \quad (2)$$

$$61 \quad f(W) = \begin{cases} \frac{1 - e^{-\theta/\theta_{sat}}}{1 - e^{-\theta_{fc}/\theta_{sat}}} & \theta \leq \theta_{fc} \\ 1.0044 - \frac{0.0044}{e^{-5 \frac{\theta/\theta_{sat} - \theta_{fc}/\theta_{sat}}{1 - \theta_{fc}/\theta_{sat}}}} & \theta \geq \theta_{fc} \end{cases} \quad (3)$$

$$62 \quad f(clay) = 1 - \frac{0.75 P_{clay}}{100} \quad (4)$$

$$f(NM) = \begin{cases} 1 - \frac{0.2 avn - avn_{opt}}{avn_{opt}} & avn > avn_{opt} \\ 1 & avn_{opt}/2 \leq avn \leq avn_{opt} \\ 1 - \frac{0.5 avn_{opt} - avn}{avn_{opt}} & avn \leq avn_{opt}/2 \end{cases} \quad (5)$$

$$f(NI) = 0.8 + \frac{0.2 avn}{avn_{opt}} \quad (6)$$

65 where k_{C_Pool} denotes the specific decomposition rate (day^{-1}); k_{max} represents the maximum decay
66 rate (day^{-1}); $f(T)$ denotes the average soil temperature scalar; $f(W)$ is the soil moisture
67 scalar; $f(\text{clay})$ is the soil texture scalar; $f(NM)$ and $f(NI)$ represent nitrogen scalars in mobilization
68 and immobilization, respectively; T is daily mean air temperature ($^{\circ}\text{C}$); θ is soil water content
69 (mm); θ_{sat} represents soil water content at field capacity (mm); θ_{fc} denotes soil water content at
70 field capacity at wilting point (mm); P_{clay} is the fraction of clay in soil (%); avn is the available
71 nitrogen in the soil (g N m^{-2}); and avn_{opt} is the optimum available nitrogen in the soil (g N m^{-2}).
72 More detail information can be found in Tian et al. (2015).

73 **2. Carbon loadings from terrestrial ecosystem to streams**

74 In DLEM 2.0, we simulate the DOC within soil. The desorption and absorption processes of
75 litter and soil organic matter pools control the soil DOC level (Chantigny, 2003). The terrestrial
76 DOC yield is simulated with:

$$R_{lchdoc} = SDOC \times fflow \times \frac{DOCC}{DOCC + lchb_{doc}} \quad (7)$$

78 where R_{lchdoc} is the export rate of dissolved organic carbon ($\text{g C m}^{-2} \text{d}^{-1}$), SDOC is the total
79 amount of dissolved organic carbon in soil (g C m^{-2}), fflow is the runoff coefficient for export
80 (unitless), $DOCC$ is the concentration of dissolved organic carbon ($\text{g C g soil}^{-1} \text{d}^{-1}$), and $lchb_{doc}$ is
81 the soil desorption coefficient for DOC ($\text{g C g soil}^{-1} \text{d}^{-1}$).

82 Here we assume loading of POC is linearly correlated with soil erosion, and the soil erosion rate
83 is based on the Modified Universal Soil Loss Equation (Williams & Berndt, 1977):

$$84 \quad R_{lchpoc} = T_{occ} \times R_{erosion} \quad (8)$$

85 where R_{lchpoc} is the rate of particulate organic carbon production in conjunction with soil erosion
86 ($\text{g C m}^{-2} \text{d}^{-1}$), T_{occ} is the concentration of total organic carbon in soil column (g C g soil^{-1}),
87 and $R_{erosion}$ is the soil erosion rate ($\text{g soil m}^{-2} \text{d}^{-1}$).

88 Export of DIC in DLEM 2.0 includes three processes: dissolution of atmospheric CO_2 ,
89 dissolution of soil CO_2 , and carbonate rock weathering. We assume dissolution of atmospheric
90 CO_2 to be the primary source of DIC in surface runoff, and we simulate this process according to
91 Henry's law. Carbon dioxide dissolution includes two reactions. The first reaction is the process
92 in which free CO_2 enters water and becomes dissolved CO_2 and H_2CO_3 , which collectively are
93 referred to as H_2CO_3^* . The second reaction is the dissociation of H_2CO_3^* to HCO_3^- and H^+ . The
94 amount of dissolved CO_2 is calculated with:

$$95 \quad [\text{H}_2\text{CO}_3^*] = K_h \times p\text{CO}_2 \quad (9)$$

96 where the brackets indicate concentration (M), $p\text{CO}_2$ is the partial pressure of atmospheric
97 CO_2 (atm), and K_h is the Henry's law equilibrium coefficient ($M \text{ atm}^{-1}$).

98 Another important source of DIC is soil carbonate weathering, which was modeled using
99 (Holford & Mattingly, 1975; Plummer et al., 1978):

$$100 \quad WR_{co3} = R_{co3} \times S_{area} \quad (10)$$

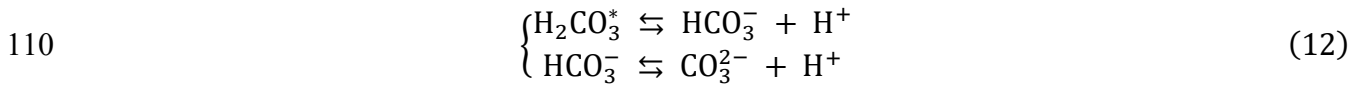
101 where WR_{co3} is the weathering rate of soil carbonate rock ($\text{g C m}^{-2} \text{s}^{-1}$), R_{co3} is the specific
102 weathering rate per unit area of carbonate rock ($\text{g C m}^{-2} \text{s}^{-1}$), and S_{area} is the surface area ratio of
103 carbonate rock in the soil ($\text{m}^2 \text{ carbonate m}^{-2} \text{ soil}$).

104 3. Inorganic carbon chemistry

105 After carbon dioxide dissolves into water, it reacts with water to form three carbon species:
106 including carbon dioxide (H_2CO_3^*), bicarbonate ion (HCO_3^-), and carbonate ion (CO_3^{2-}). The sum
107 of these three species is dissolved inorganic carbon:

$$108 \quad [\text{DIC}] = [\text{HCO}_3^-] + [\text{H}_2\text{CO}_3^*] + [\text{CO}_3^{2-}] \quad (11)$$

109 The chemical reactions are:



111 The equilibrium constants (K_1 and K_2) for the combined reactions can be used to determine the
112 proportion of carbon species:

$$113 \quad pK_1 = \frac{3404.71}{T_w} + 0.032786T_w - 14.8435 \quad (13)$$

$$114 \quad pK_1 = \frac{[\text{H}^+][\text{HCO}_3^-]}{[\text{H}_2\text{CO}_3^*]} \quad (14)$$

$$115 \quad pK_2 = \frac{2902.39}{T_w} + 0.02379T_w - 6.498 \quad (15)$$

$$116 \quad pK_2 = \frac{[\text{H}^+][\text{CO}_3^{2-}]}{[\text{HCO}_3^-]} \quad (16)$$

117 where K_1 is composite acidity constant of H_2CO_3^* , K_2 is the second dissociation constant of
118 carbonic acid, T_w is water temperature ($^\circ\text{C}$), and $[\text{H}^+]$ is the concentration of H^+ , which is
119 derived from the temporally constant pH value that is spatially interpolated from observations
120 (Supplementary Figure 1). In our current model version, we did not consider the balance of
121 charge or electroneutrality that involves alkalinity because it is unnecessary if the pH is known.
122 That is, given $[\text{H}^+]$ and $[\text{DIC}]$, Equations 11, 14, and 16 can be used to compute $[\text{H}_2\text{CO}_3^*]$
123 because there are only two other unknowns, $[\text{HCO}_3^-]$ and $[\text{CO}_3^{2-}]$.

124 Supplementary Table 1. USGS sites selected for model evaluation

<i>Rivers</i>	<i>Locations</i>	<i>USGS Gauge Stations</i>
Delaware River	Trenton NJ	01463500
Delaware River	Montague NJ	01438500
Susquehanna River	Conowingo, MD	01578310
Susquehanna River	Danville, PA	01540500
Susquehanna River	Harrisburg, PA	01570500
Patuxent River	Bowie, MD	01594440
York River	Hanover, VA	01673000
Rappahannock River	Fredericksburg, VA	01668000
James River	Cartersville, VA	02035000

125

126

127

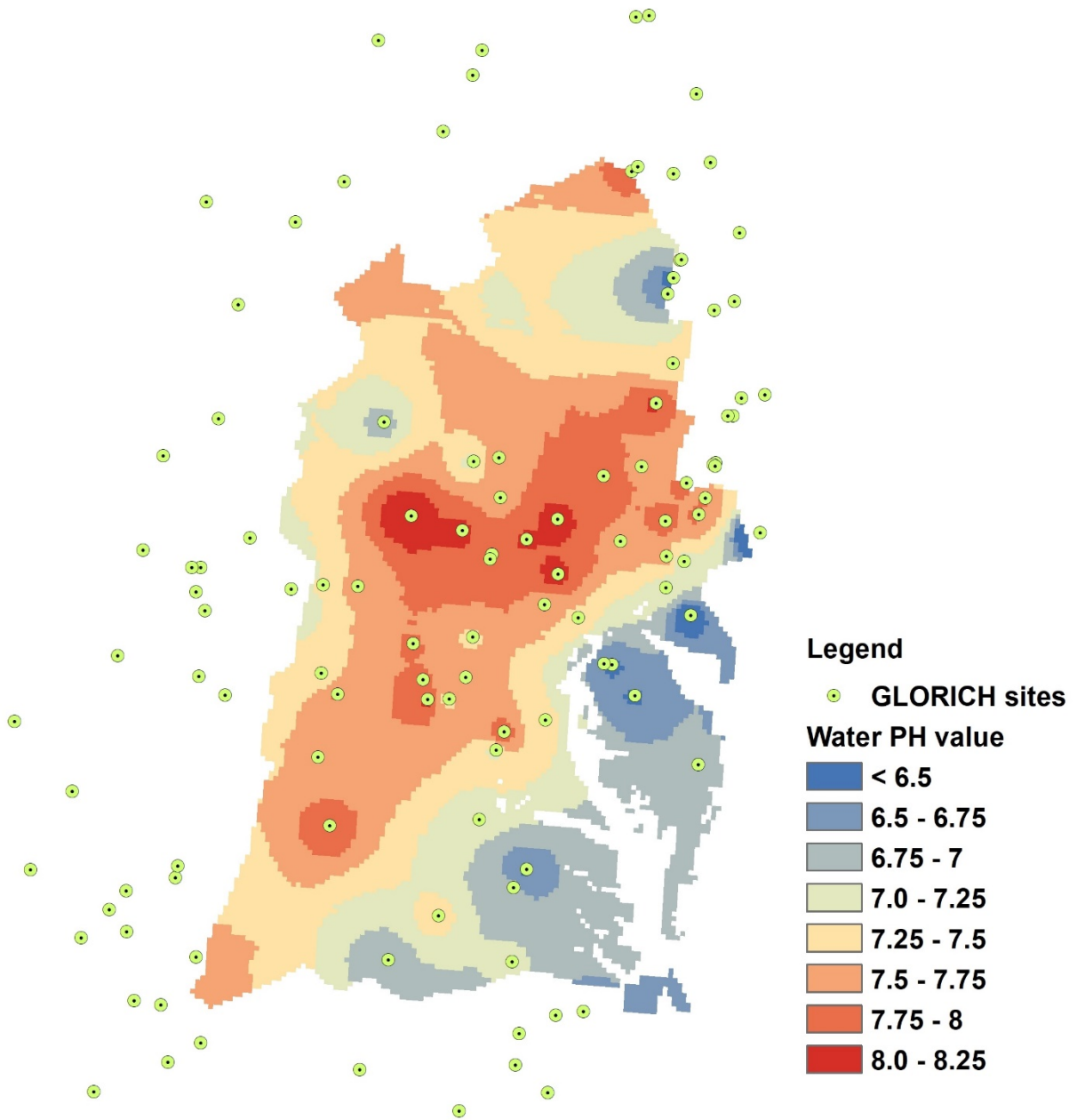
128

129 Supplementary Table 2. Carbon Export-Related Parameters in the Dynamic Land Ecosystem
 130 Model (DLEM 2.0)

Parameters	Unit	Values in DLEM 2.0	Range from previous studies	Reference
$f_{\text{doc-dec}}$	unitless	0.1–0.5	0.05–0.21	(Park et al., 2002)
lchb_{doc}	g C g soil^{-1}	1×10^{-9} – 3×10^{-6}	0–0.00078	(Neff & Asner, 2001)
K_{DOC}	day^{-1}	0.002	0.0006–0.0055	(Koehler et al., 2012)
K_{POC}	day^{-1}	0.005	0.008	(Enríquez et al., 1993)
Q_{10}	unitless	2	1.47–2.88	(Kätterer et al., 1998)
R_{flow}	unitless	2	1–10	from the USGS gauge record
$kaom1$	day^{-1}	0.0005–0.009	0.002–0.005	(Petersen et al., 2005)
$kaom2$	day^{-1}	0.005–0.1	0.025–0.06	(Petersen et al., 2005)
$esmb$	day^{-1}	0.4–0.6	0.6	(Hansen et al., 1991)
$knom$	day^{-1}	0.000146	0.000113–0.000146	(Petersen et al., 2005)
$ksmr$	day^{-1}	0.0044	0.0044	(Petersen et al., 2005)
ps	$(\text{g}\cdot\text{cm}^{-3})$	1.1	1.02–1.27	(Thomann & Mueller, 1987)
α (shape factor)	unitless	1	1	(Thomann & Mueller, 1987)

131• Note: we calibrate lchb_{doc} for different plant functional types to ensure the simulated carbon
 132 fluxes match the water quality estimation given by the LOADEST estimator. $kaom1$: decay rate
 133 of fast litter pool; $kaom2$: decay rate of slow litter pool; $esmb$: fraction of incoming carbon for
 134 microbial mass pools utilized by microbial; $knom$: decay rate of native organic matter; and $ksmr$:
 135 decay rate of microbial mass residual.

136

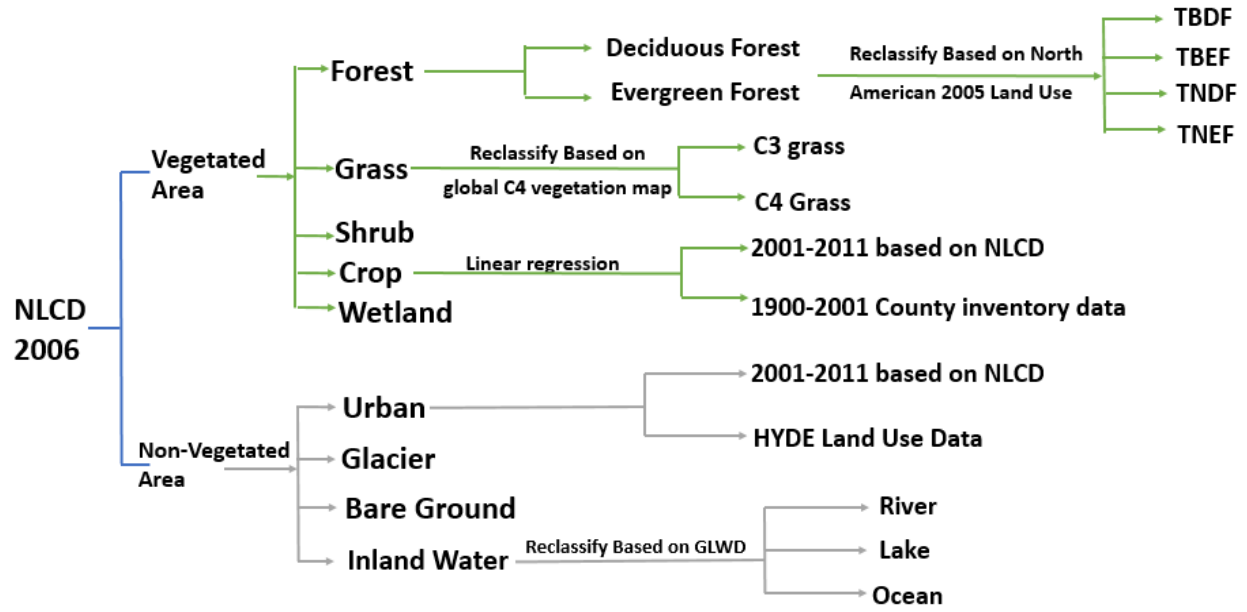


137
138

139 Supplementary Figure 1. The spatial map of water pH interpolated from long-term observations
140 of the GLORICH database. Note: We selected 115 GLORICH sites within or surrounding the
141 Chesapeake and Delaware Bay Watersheds. We first averaged pH at each site from 1979 to 2015
142 and then interpolated the averaged pH values to create the spatial pH map, which was used as
143 DLEM model input.

144

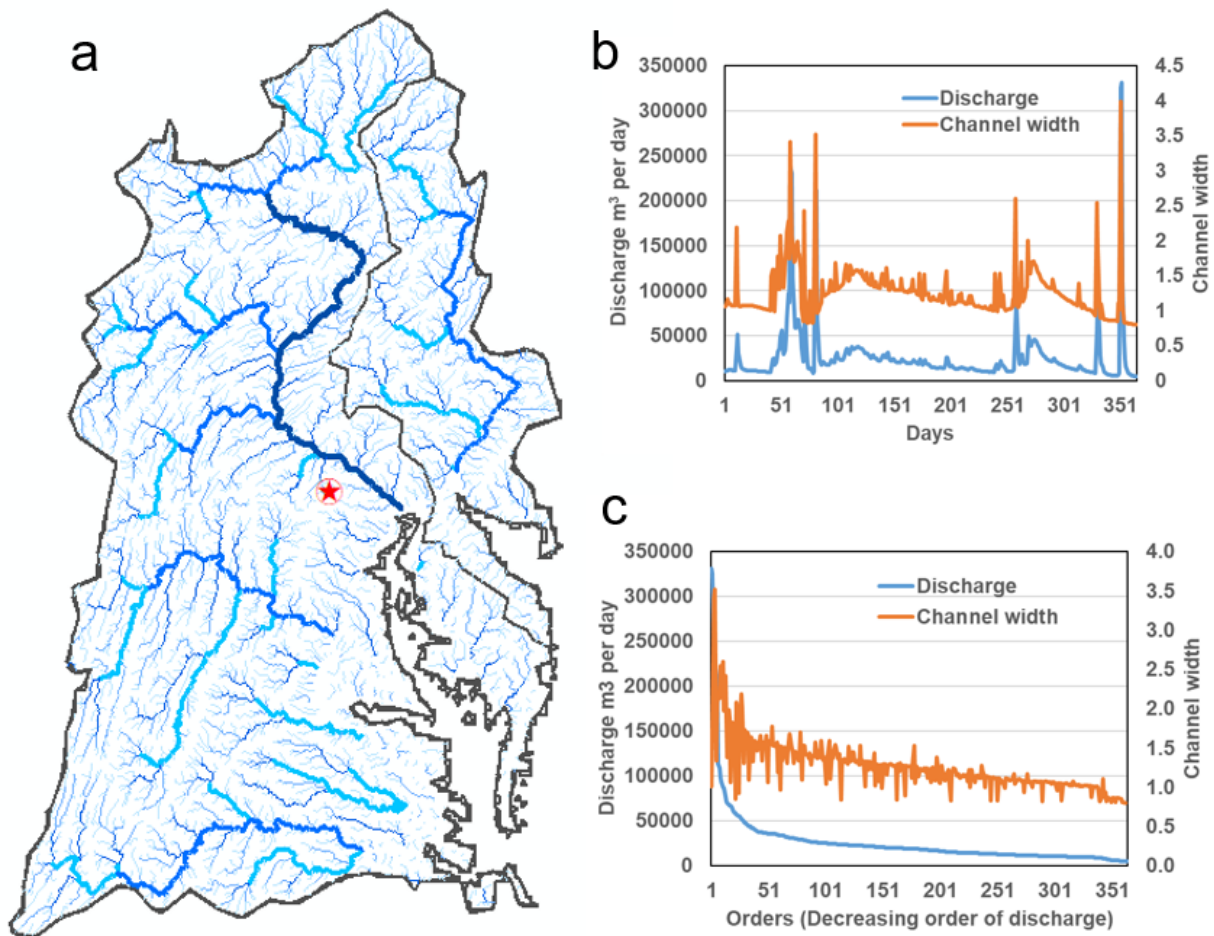
145
146
147



148

149 Supplementary Figure 2. The flowchart to describe the development of historical land-use cohort

150
151
152
153



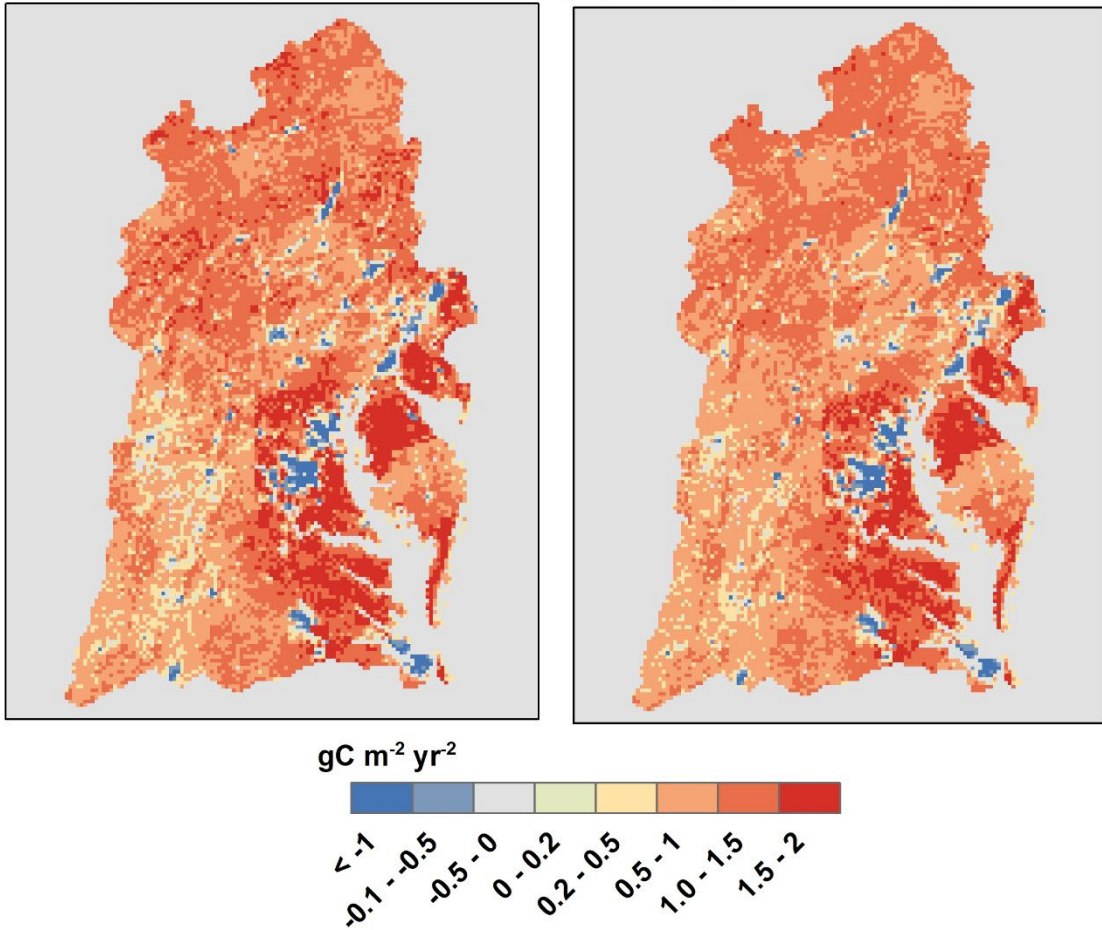
154

155 Supplementary Figure 3. Width changes at-a-site during storms in the year 2000. (a) the location
 156 of the site, with the drainage area equal to 16km^2 . (b) the simulated flow discharge (m^3/day) and
 157 channel width (m) from during the year 2000. (c) the sorted discharge in decreasing order and
 158 the associated channel width.

159

(a) Changes in NPP

(b) Changes in soil respiration



160

161 Supplementary Figure 4. Spatiotemporal patterns of changes in NPP (a) and soil respiration (b)
162 from 1900 to 2015.

163

164 **Reference**

165 Chantigny, M. H. (2003). Dissolved and water-extractable organic matter in soils: A review on
166 the influence of land use and management practices. *Geoderma*, 113(3–4), 357–380.

167 Enríquez, S., Duarte, C. M., & Sand-Jensen, K. A. J. (1993). Patterns in decomposition rates
168 among photosynthetic organisms: The importance of detritus C: N: P content. *Oecologia*,
169 94(4), 457–471.

170 Hansen, S., Jensen, H. E., Nielsen, N. E., & Svendsen, H. (1991). Simulation of nitrogen
171 dynamics in the soil-plant system using the danish simulation model DAISY,
172 Hydrological interactions between atmosphere. *Soil Veg*, 204, 185–196.

173 Holford, I. C. R., & Mattingly, G. E. G. (1975). Surface areas of calcium carbonate in soils.
174 *Geoderma*, 13(3), 247–255.

175 Kätterer, T., Reichstein, M., Andrén, O., & Lomander, A. (1998). Temperature dependence of
176 organic matter decomposition: A critical review using literature data analyzed with
177 different models. *Biology and Fertility of Soils*, 27(3), 258–262.

178 Koehler, B., von Wachenfeldt, E., Kothawala, D., & Tranvik, L. J. (2012). Reactivity continuum
179 of dissolved organic carbon decomposition in lake water. *Journal of Geophysical*
180 *Research: Biogeosciences*, 117(G1).

181 Neff, J. C., & Asner, G. P. (2001). Dissolved organic carbon in terrestrial ecosystems: Synthesis
182 and a model. *Ecosystems*, 4(1), 29–48.

183 Park, J.-H., Kalbitz, K., & Matzner, E. (2002). Resource control on the production of dissolved
184 organic carbon and nitrogen in a deciduous forest floor. *Soil Biology and Biochemistry*,
185 34(6), 813–822.

186 Petersen, B. M., Berntsen, J., Hansen, S., & Jensen, L. S. (2005). CN-SIM—a model for the
187 turnover of soil organic matter. I. Long-term carbon and radiocarbon development. *Soil*
188 *Biology and Biochemistry*, 37(2), 359–374.

189 Plummer, L. N., Wigley, T. M. L., & Parkhurst, D. L. (1978). The kinetics of calcite dissolution
190 in CO₂-water systems at 5 degrees to 60 degrees C and 0.0 to 1.0 atm CO₂. *American*
191 *Journal of Science*, 278(2), 179–216.

192 Tian, H., Chen, G., Zhang, C., Liu, M., Sun, G., Chappelka, A., Ren, W., Xu, X., Lu, C., Pan, S.,
193 Chen, H., Hui, D., McNulty, S., Lockaby, G., & Vance, E. (2012). Century-Scale
194 Responses of Ecosystem Carbon Storage and Flux to Multiple Environmental Changes in
195 the Southern United States. *Ecosystems*, 15(4), 674–694. [https://doi.org/10.1007/s10021-](https://doi.org/10.1007/s10021-012-9539-x)
196 [012-9539-x](https://doi.org/10.1007/s10021-012-9539-x)

197 Tian, H., Yang, Q., Najjar, R. G., Ren, W., Friedrichs, M. A. M., Hopkinson, C. S., & Pan, S.
198 (2015). Anthropogenic and climatic influences on carbon fluxes from eastern North
199 America to the Atlantic Ocean: A process-based modeling study. *Journal of Geophysical*
200 *Research: Biogeosciences*, 120(4), 757–772. <https://doi.org/10.1002/2014JG002760>

201 Williams, J. R., & Berndt, H. D. (1977). Sediment yield prediction based on watershed
202 hydrology. *Transactions of the ASAE*, 20(6), 1100–1104.

203

204